

Differential activation and modulation of the glucagon-like peptide-1 receptor by small molecule ligands

Wootten D, Savage EE, Willard FS, Bueno AB, Sloop KW, Christopoulos A, Sexton PM

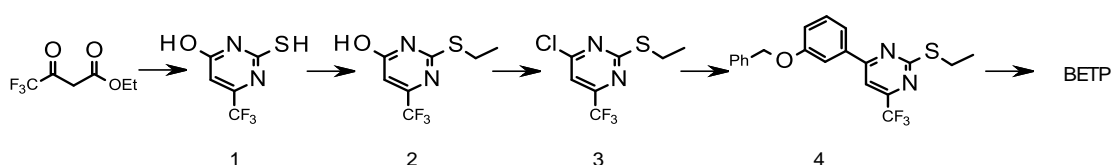
Molecular Pharmacology

Supplemental Information

Experimental procedure.

General synthesis. All chemicals were reagent grade and used as purchased. Flash chromatography was performed in Biotage Radial Compression system or flash chromatography using Merck silica gel 60 mesh. Eluents are indicated for each compound. ^1H NMR and ^{13}C NMR spectra were recorded in δ units relative to deuterated solvent as an internal reference using a Varian 400 MHz NMR or a Bruker 300 MHz NMR instrument. Signal multiplicities are represented by s (singlet), d (doublet), t (triplet), q (quartet), bs (broad singlet), and m (multiplet). HPLC/MS was used for the determination of reaction conversion on a series 1100 liquid chromatography/mass selective detector LC/MSD (Agilent, Waldbronn, Germany) driven by ChemStation software (Rev. A10.02, Agilent Technologies). LC/UV analysis was carried out at low or high pH. Conditions for low pH: Column: Gemini C18 3 μm (2 x 50 mm); UV: 214 and 300; eluent: A: 0.1% H₂O-formic acid pH 2.7, B: acetonitrile-formic acid 0.1%; flow: 1 ml/min; T: 50°C; gradient: from 5 to 100% B in 7 min. Conditions for high pH: Column: Xbridge C18 3.5 μm (2.1 x 50 mm); UV: 214 and 300; eluent: A: 10mM ammonium bicarbonate pH 9, B: acetonitrile; flow: 1 ml/min; T: 50°C; gradient: from 10 to 100% B in 7 min.

BETP synthesis



2-Mercapto-6-trifluoromethyl-pyrimidin-4-ol (1) A solution of ethyl 4,4,4-trifluoro-3-oxobutanoate (100 g, 543.14 mmol) and thiourea (100 g, 131.0 mmol) was suspended in 1.2 L of methanol. Sodium methoxide (68 g, 126.0 mmol) was added in portions over a 5 minute period (the temperature rose from 23°C to 44°C during addition). The mixture was refluxed overnight. The cooled solution was concentrated to ~1/3 volume, transferred to a separatory funnel, acidified to pH 2 with 12N HCl, and extracted with *t*-butylmethylether (2 x 2 L). The organic layers were washed with water and brine, dried (MgSO₄), filtered, and the filtrate evaporated to provide 2-mercapto-6-trifluoromethyl-pyrimidin-4-ol (79 g, 74% yield). LCMS m/z 197 [M+1]; ¹H NMR (400 MHz, DMSO-d₆) δ-6.38 (s, 1H); ¹⁹F NMR (376 MHz, DMSO-d₆) □ -68.1 (s, CF₃).

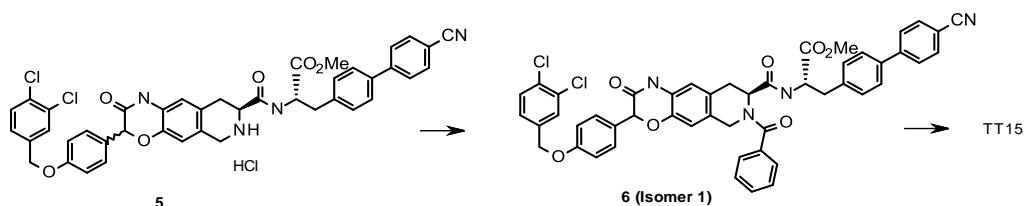
2-Ethylsulfanyl-6-trifluoromethyl-pyrimidin-4-ol (2) A solution of 2-mercapto-6-trifluoromethyl-pyrimidin-4-ol (79 g, 402.75 mmol) was dissolved in 800 mL of DMSO and treated with potassium carbonate (56 g, 405.19 mmol), followed by iodoethane (62 g, 397.52 mmol) in portions over a five minute period. The temperature gently rose from ambient to 38°C after addition. After stirring overnight at room temperature, the mixture was poured into water (4 L), the pH adjusted to ~2 with 12 N HCl and extracted with ethyl acetate (2 x 2 L). The organic extracts were washed with water and brine, dried (MgSO₄), filtered, and the filtrate evaporated to provide 2-ethylsulfanyl-6-trifluoromethyl-pyrimidin-4-ol (88.6 g, 98% yield) as an off white solid. LCMS m/z 223 [M-1]; ¹H NMR (400 MHz, DMSO-d₆) δ-13.27 (bs, 1H), 6.55 (s, 1H), 3.08 (q, *J* = 7.4 Hz, 2H), 1.26 (t, *J* = 7.4 Hz, 3H); ¹⁹F NMR (376 MHz, DMSO-d₆) δ-70.5 (s, CF₃).

4-Chloro-2-ethylsulfanyl-6-trifluoromethyl-pyrimidine (3) A slurry of 2-ethylsulfanyl-6-trifluoromethyl-pyrimidin-4-ol (88.6 g, 395.17 mmol) was combined with phosphoryl chloride (500 mL, 538.0 mmol), treated with dimethylformamide (2 mL, 25.87 mmol), and gently refluxed for 2 hours. The phosphoryl chloride was evaporated off, and the residue slowly poured in vigorously stirred water (1 L) at room temperature over a 20 minute period. After stirring 2 hours, the mixture was transferred to a separatory funnel and extracted with ethyl acetate (2 x 750 mL). The organic layers were washed with water, saturated sodium bicarbonate and brine, dried (MgSO₄), filtered, and the filtrate evaporated to provide

4-chloro-2-ethylsulfanyl-6-trifluoromethyl-pyrimidine (74 g, 77% yield) as an oily yellow solid. ^1H NMR (400 MHz, DMSO- d_6) δ -7.94 (s, 1H), 3.08 (q, J = 7.4 Hz, 2H), 1.26 (t, J = 7.4 Hz, 3H); ^{19}F NMR (376 MHz, DMSO- d_6) δ -68.0 (s, CF_3).

4-(3-Benzyloxy-phenyl)-2-ethylsulfanyl-6-trifluoromethyl-pyrimidine (4) To a solution of 3-benzyloxyphenylboronic acid (25 g, 109.62 mmol) and 4-chloro-2-ethylsulfanyl-6-trifluoromethyl-pyrimidine (15 g, 61.82 mmol) was added 1,4-dioxane (600 mL) and water (120 mL). Sodium carbonate (14 g, 132.09 mmol) was then added and the mixture was degassed via nitrogen flow through a glass gas dispersion tube for 20 min. The reaction was stirred overnight at 80 °C. The cooled mixture was diluted with water (1.5 L) and extracted with ethyl acetate (2 x 1 L). The black organic layers were washed with water and brine, dried (MgSO_4), filtered, and the filtrate evaporated. The crude was purified by chromatography on silica gel eluting with hexanes followed by 20% dichloromethane in hexanes to afford 4-(3-benzyloxy-phenyl)-2-ethylsulfanyl-6-trifluoromethyl-pyrimidine (12.5 g, 52% yield) as a colorless oil. LCMS m/z 391 [$\text{M}+1$]; ^1H NMR (400 MHz, DMSO- d_6) δ -8.22 (s, 1H), 7.90-7.88 (m, 2H), 7.50-7.24 (m, 7H), 5.20 (s, 2H), 3.20 (q, J = 7.0 Hz, 2H), 1.36 (t, J = 7.0 Hz, 3H); ^{19}F NMR (376 MHz, DMSO- d_6) δ -68.3 (s, CF_3).

4-(3-Benzyloxyphenyl)-2-[ethylsulfinyl]-6-(trifluoromethyl)pyrimidine (BETP) A solution of 4-(3-benzyloxy-phenyl)-2-ethylsulfanyl-6-trifluoromethyl-pyrimidine (9.5 g, 20.93 mmol) was dissolved in methanol (400 mL) and poured into water (80 mL) under nitrogen. Potassium monopersulfate (7.4 g, 12.04 mmol) was added and the mixture was stirred overnight at room temperature. The mixture was concentrated to ~1/3 volume, diluted with water, and extracted with ethyl acetate (2 x 200 mL). The organic layers were dried (MgSO_4), filtered, and the filtrate evaporated. The crude material was purified by flash chromatography on silica gel eluting with 1:2 ethyl acetate/hexane to provide racemic 4-(3-benzyloxyphenyl)-2-[ethylsulfinyl]-6-(trifluoromethyl)pyrimidine (7 g, 82% yield) as a white solid. LCMS m/z 407 [$\text{M}+1$]; ^1H NMR (400 MHz, DMSO- d_6) δ -8.69 (s, 1H), 7.98 (m, 2H), 7.53-7.29 (m, 7H), 5.21 (s, 2H), 3.28 (m, 1H), 3.17 (m, 1H), 1.13 (m, 3H); ^{19}F NMR (376 MHz, DMSO- d_6) δ -68.1 (s, CF_3); ^{13}C NMR (300 MHz, DMSO- d_6) δ 173.2, 166.5, 158.5, 155.9 (c, J = 36 Hz), 136.2, 134.9, 130.0, 127.9, 127.4, 127.3, 120.1, 119.0, 113.6, 113.4 (c, J = 2 Hz), 69.1, 46.0, 5.3; CF_3 not detected due to low signal to noise.

TT15 synthesis

Methyl (2S)-2-[[[(8S)-7-benzoyl-3-[4-[(3,4-dichlorophenyl)methoxy]phenyl]-2-oxo-1,6,8,9-tetrahydropyrido[4,3-g][1,4]benzoxazine-8-carbonyl]amino]-3-[4-(4-cyanophenyl)phenyl]propanoate (6). Compound **5** corresponds to Intermediate A described in Rao, 2009 and was synthesized according to this procedure. Compound **5** (4.2 g, 5.26 mmol) was dissolved in dichloromethane (85 mL), triethylamine (2.24 mL, 15.7 mmol) was added under nitrogen and the solution was cooled to 0°C. Benzoyl chloride (0.88 g, 6.31 mmol) was slowly added and the reaction was allowed to warm to room temperature for 4h. Water was added (100 mL) and the reaction mixture was stirred vigorously. Layers were separated and the organic layer was washed with brine, dried (Na₂SO₄), filtered and concentrated. The crude material was purified by flash chromatography eluting with ethyl acetate/hexane (from 0:100 to 80:20) to provide 4g of a mixture of diastereoisomers. Chiral separation of diastereomers (chiral HPLC conditions: 8x31 cm Chiralcel OD, 20 μm; eluent: 90/10 MeOH/acetonitrile; flow: 400 ml/min) provided 3.1g of compound **6** (isomer 1) in 94% purity.

(2S)-2-[[[(8S)-7-benzoyl-3-[4-[(3,4-dichlorophenyl)methoxy]phenyl]-2-oxo-1,6,8,9-tetrahydropyrido[4,3-g][1,4]benzoxazine-8-carbonyl]amino]-3-[4-(4-cyanophenyl)phenyl]propanoic acid (TT15). Compound **6** (3.8 g, 3.6 mmol) was dissolved in tetrahydrofuran (200 mL) and lithium hydroxide (21.5 g, 35.6 mmol) was added. The mixture was stirred at room temperature overnight. 1N hydrochloric acid was added to pH 2 and the mixture was concentrated. The crude material was purified by reverse phase chromatography to provide 1.2 g of **TT15** as a white solid in 95% purity. LCMS m/z 851 [M+1]; ¹H NMR (300 MHz, DMSO-d₆, 100°C) δ 7.76 and 7.68 (AA'BB' system, 4H), 7.59 (m, 1H), 7.53 and 7.12 (AA'BB' system, 4H), 7.42-7.27 (m, 10H), 6.92 (m, 2H), 6.77 (s, 1H), 6.58 (bs, 1H), 6.56 (s, 1H), 5.10 (bs, 2H), 5.02 (s, 2H), 4.28 (m, 1H), 4.13 (m, 1H), 3.17-

2.95 (m, 4H); ^{13}C NMR (300 MHz, DMSO- d_6 , 100°C) δ 171.6, 170.1, 168.2, 164.3, 157.9, 144.2, 140.6, 138.7, 137.7, 135.7, 135.4, 131.9 (2C), 130.8, 130.0, 129.4, 128.9, 128.7, 128.4, 128.2, 127.8, 127.0, 126.9, 126.6, 126.3, 126.1, 125.8, 125.5, 118.1, 114.7, 114.6, 113.3, 109.3, 77.2, 67.7, 53.8 (2C), 40.4, 36.2, 29.0.

Boc-5, **Compound 2** and **BMS21** were synthesized according to the methods described in the literature (Chen *et al*, 2007; Teng *et al*, 2007; Mapelli *et al*, 2009). The structures of all new compounds were consistent with their ^1H and mass spectra, and were $\geq 95\%$ pure as measured by HPLC.

- Chen D, Liao J, Li N, Zhou C, Liu Q, Wang G, Zhang R, Zhang S, Lin L, Chen K, Xie X, Nan F, Young AA and Wang MW (2007) A nonpeptidic agonist of glucagon-like peptide 1 receptors with efficacy in diabetic db/db mice. *Proc Natl Acad Sci U S A* **104**(3):943-948.
- Mapelli C, Natarajan SI, Meyer JP, Bastos MM, Bernatowicz MS, Lee VG, Pluscec J, Riexinger DJ, Sieber-McMaster ES, Constantine KL, Smith-Monroy CA, Golla R, Ma Z, Longhi DA, Shi D, Xin L, Taylor JR, Koplowitz B, Chi CL, Khanna A, Robinson GW, Seethala R, Antal-Zimanyi IA, Stoffel RH, Han S, Whaley JM, Huang CS, Krupinski J and Ewing WR (2009) Eleven amino acid glucagon-like peptide-1 receptor agonists with antidiabetic activity. *J Med Chem* **52**(23):7788-7799.
- Rao M (2009) PCT/US2009/039905 "Ligands for the Glp-1 Receptor and methods for discovery thereof", I.P. Application, Editor, TransTech Pharma.
- Teng M, Johnson MD, Thomas C, Kiel D, Lakis JN, Kercher T, Aytes S, Kostrowicki J, Bhumralkar D, Truesdale L, May J, Sidelman U, Kodra JT, Jørgensen AS, Olesen PH, de Jong JC, Madsen P, Behrens C, Pettersson I, Knudsen LB, Holst JJ, Lau J (2007) Small molecule allosteric modulators of the human glucagon like peptide-1 (hGLP-1) receptor. *Bioorg Med Chem Lett* **17** (19) 5472–5478.

Figure legends

Supplementary figure 1. Competition binding assays.

Characterisation of the binding of (A) TT15, (B) BMS21 (D) Boc5, (E) BETP and (F) Compound 2 in competition with the radiolabeled antagonist, ^{125}I -exendin(9–39), in whole FlpInCHO cells stably expressing the human GLP-1R. On all graphs competition binding between the control ligand GLP-1(7-36) NH_2 and the radioligand are also shown. Data are normalized to maximum ^{125}I -exendin(9–39) binding, with nonspecific binding measured in the presence of 1 μM exendin(9–39). Data are analysed with a three-parameter logistic equation. All values are means \pm S.E.M of three to four independent experiments, conducted in duplicate.

Supplementary figure 2. BETP and Compound 2 selectively potentiate the affinity of oxyntomodulin.

Inhibition binding curves of (A, E) exendin-4, (B, F) GLP-1(7-36) NH_2 , (C, G) Oxyntomodulin and (D, H) GLP-1(1-36) NH_2 in the absence and presence of increasing concentrations of either Compound 2 (A-D) or BETP (E-H). Data are normalised to max ^{125}I -exendin(9-39) binding and are analysed with a one-site competition plus allosteric modulator curve as defined in equations 1 and 2. All values are means \pm S.E.M of three to four independent experiments, conducted in duplicate.

Supplementary figure 3. Compound 2 displays positive allosteric effects on GLP-1R-mediated cAMP accumulation in an agonist-dependent manner.

Concentration response curves were generated for (A) exendin-4, (B) GLP-1(7-36) NH_2 , (C) oxyntomodulin or (D) GLP-1(1-36) NH_2 in the absence and presence of increasing concentrations of Compound 2 in FlpInCHO cells stably expressing the human GLP-1R. The curves represent the best global fit of an operational model of allosterism (equation 4). All values are mean \pm SEM of three to four independent experiments performed in duplicate.

Supplementary figure 4. Compound 2 does not alter GLP-1R-mediated iCa^{2+} mobilisation by peptide ligands.

Concentration response curves were generated for (A) exendin-4, (B) GLP-1(7-36) NH_2 or (C) Oxyntomodulin in the absence and presence of increasing concentrations of Compound 2 in FlpInCHO cells stably expressing the human GLP-1R. The curves represent the best global fit of an operational model of allosterism (equation 4). All values are mean \pm SEM of three to four independent experiments performed in duplicate.

Supplementary figure 5. Compound 2 displays negative allosteric effects on GLP-1R-mediated pERK1/2 by peptide ligands .

Concentration response curves were generated for (A) exendin-4, (B) GLP-1(7-36) NH_2 , (C) Oxyntomodulin or (D) GLP-1(1-36) NH_2 in the absence and presence of increasing concentrations of Compound 2 in FlpInCHO cells stably expressing the human GLP-1R. The curves represent the best global fit of an operational model of allosterism (equation 5). All values are mean \pm SEM of three to four independent experiments performed in duplicate.

Supplementary figure 6. BMS21 does not modulate peptide-mediated GLP-1R signalling.

Concentration response curves were generated for exendin-4 (A, E, I), GLP-1(7-36)NH₂ (B, F, J), Oxyntomodulin (C, G, K) or GLP-1(1-36)NH₂ (D, H, L) in the absence and presence of increasing concentrations of BMS21 for cAMP accumulation (A-D), pERK1/2 (E-H) and iCa²⁺ mobilisation (I-L) in FlpInCHO cells stably expressing the human GLP-1R. Data are analysed with a three-parameter logistic equation. All values are means \pm S.E.M of three independent experiments, conducted in duplicate.

Supplementary figure 7. Boc5 displays behaviour consistent with competitive interaction with peptides in GLP-1R-mediated signalling.

Concentration response curves were generated for exendin-4 (A, E, I), GLP-1(7-36)NH₂ (B, F, J), Oxyntomodulin (C, G, K) or GLP-1(1-36)NH₂ (D, H, L) in the absence and presence of increasing concentrations of Boc5 for cAMP accumulation (A-D), pERK1/2 (E-H) and iCa²⁺ mobilisation (I-L) in FlpInCHO cells stably expressing the human GLP-1R. Data are analysed with a three-parameter logistic equation. All values are means \pm S.E.M of three independent experiments, conducted in duplicate.

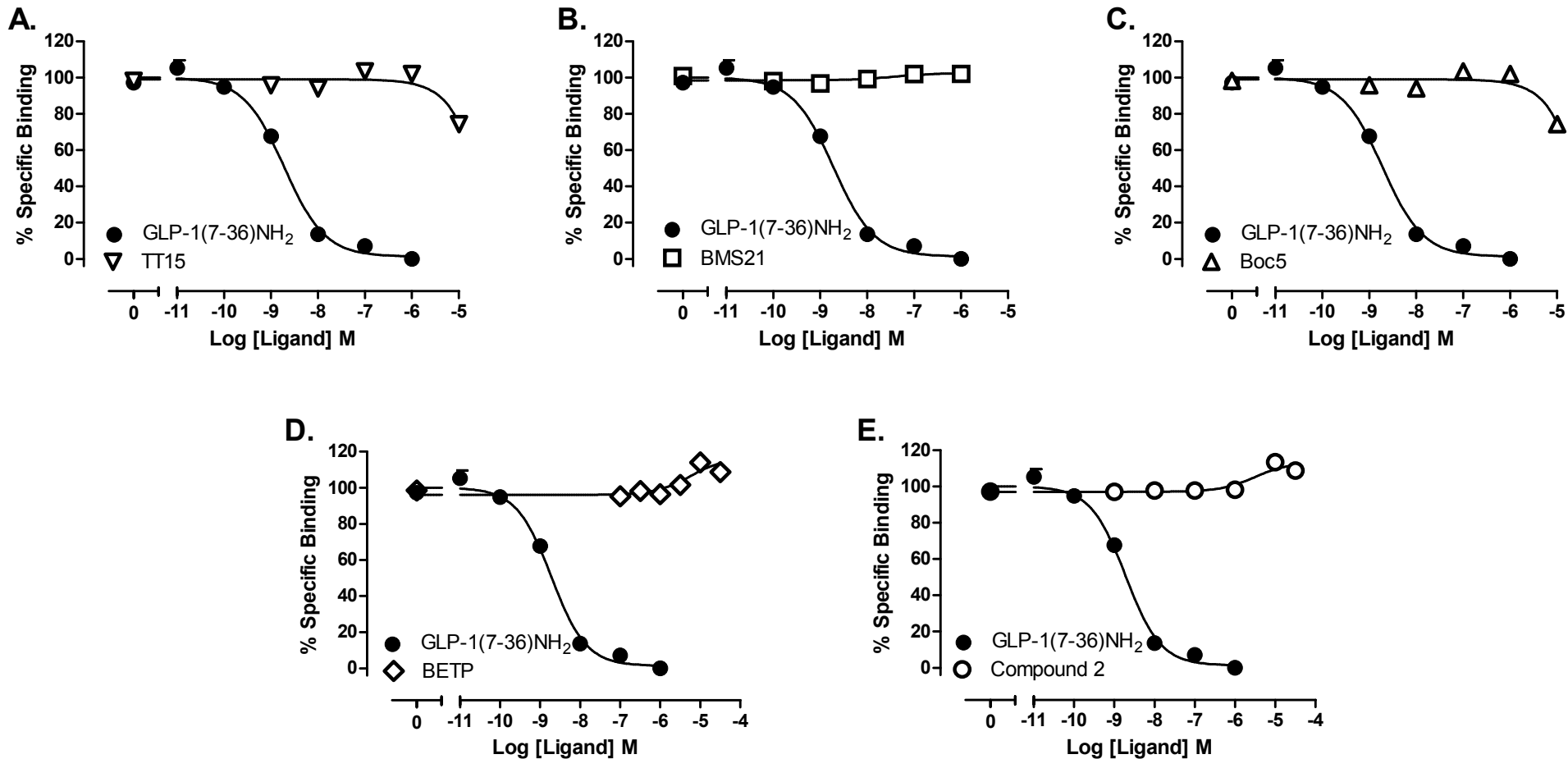
Supplementary figure 8. TT15 displays behaviour consistent with competitive interaction with peptides in GLP-1R-mediated signalling.

Concentration response curves were generated for exendin-4 (A, E, I), GLP-1(7-36)NH₂ (B, F, J), Oxyntomodulin (C, G, K) or GLP-1(1-36)NH₂ (D, H, L) in the absence and presence of increasing concentrations of TT15 for cAMP accumulation (A-D), pERK1/2 (E-H) and iCa²⁺ mobilisation (I-L) in FlpInCHO cells stably expressing the human GLP-1R. Data are analysed with a three-parameter logistic equation. All values are means \pm S.E.M of three independent experiments, conducted in duplicate.

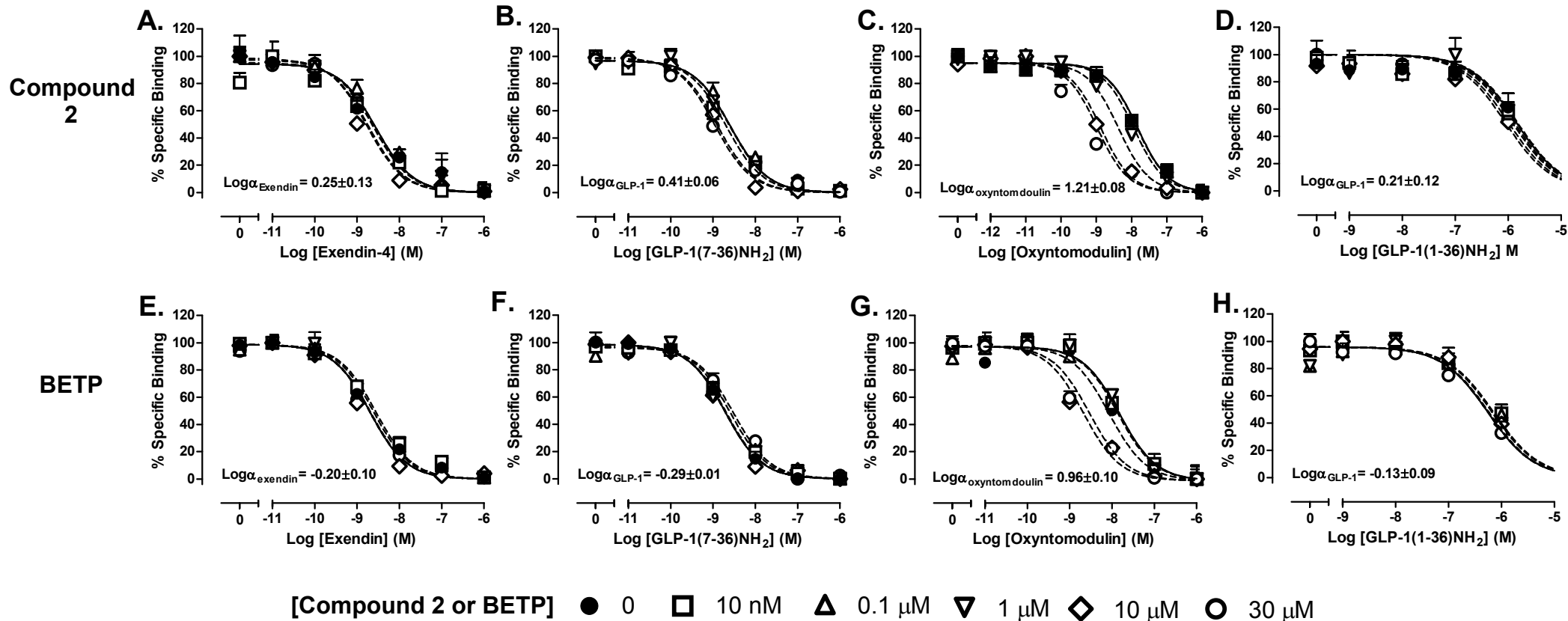
Supplementary figure 9. BMS21, Boc5 and TT15 display behaviour consistent with competitive interaction when interacted together in GLP-1R-mediated cAMP signalling.

Concentration response curves were generated for Boc5 (A, B) and TT15 (C) in the absence and presence of increasing concentrations of either TT15 (A) or BMS21 (B-C) in FlpInCHO cells stably expressing the human GLP-1R. Data are analysed with a three-parameter logistic equation. All values are means \pm S.E.M of three independent experiments, conducted in duplicate.

Supplementary figure 1

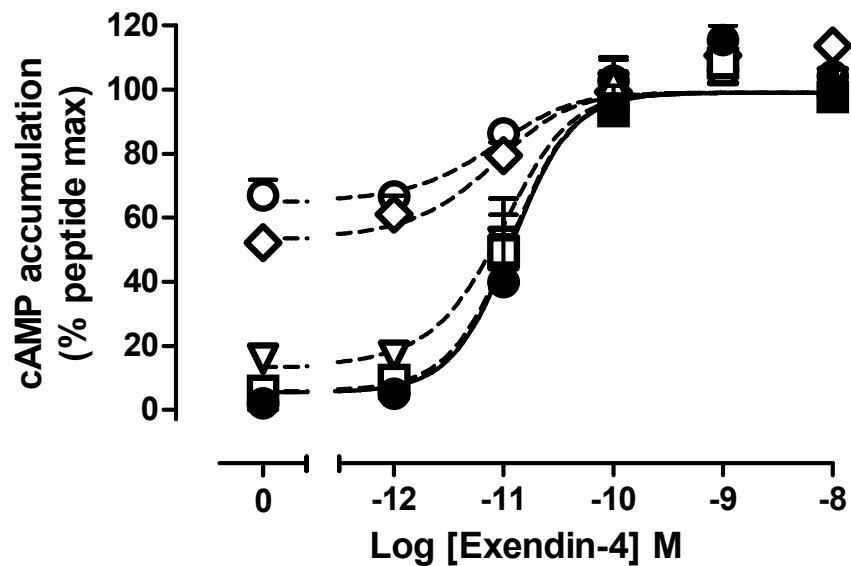


Supplementary figure 2

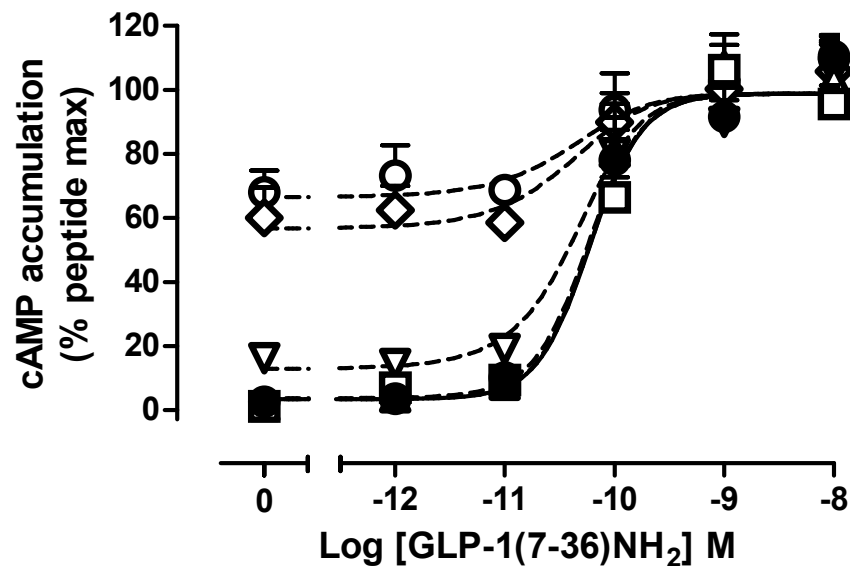


Supplementary figure 3

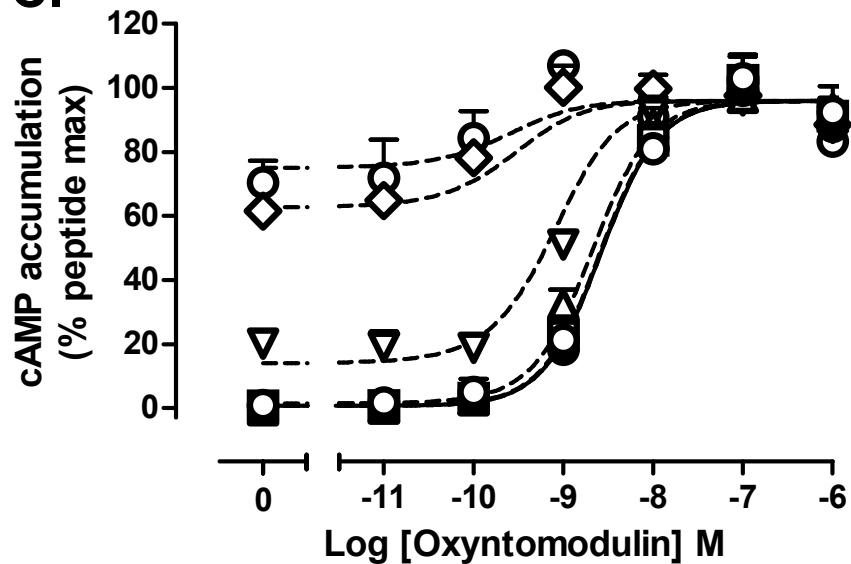
A.



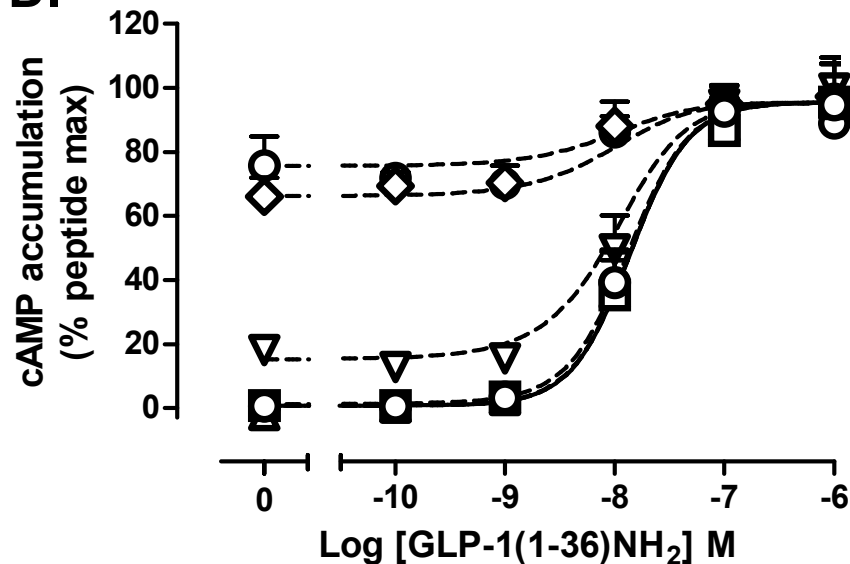
B.



C.

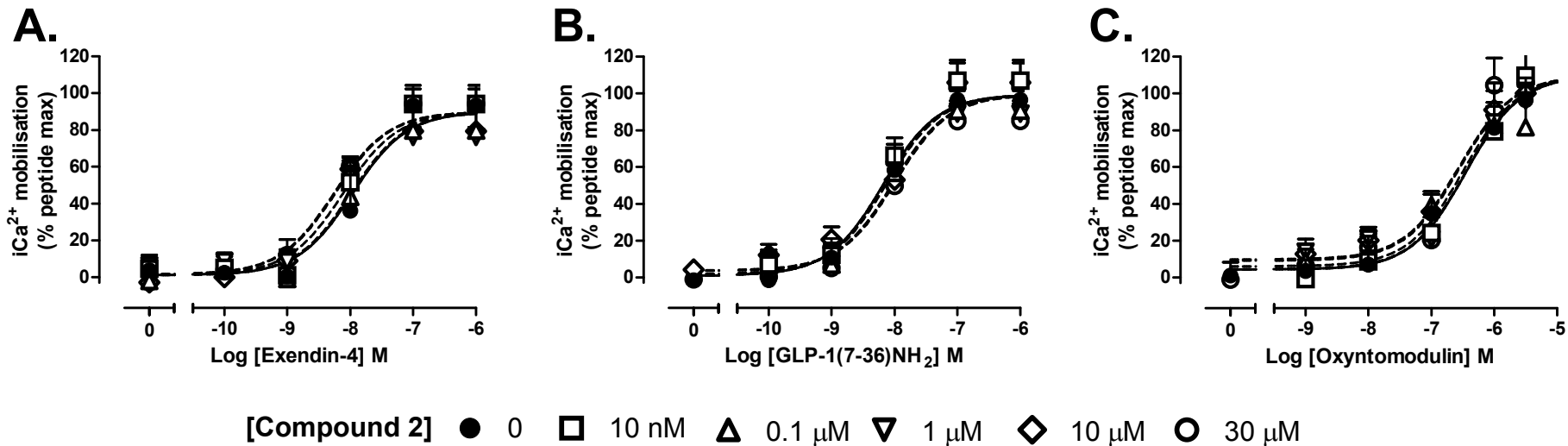


D.

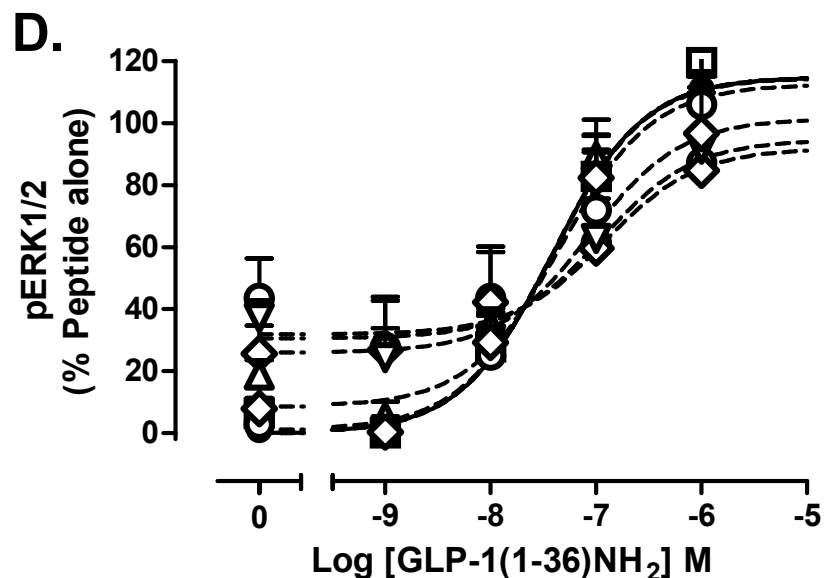
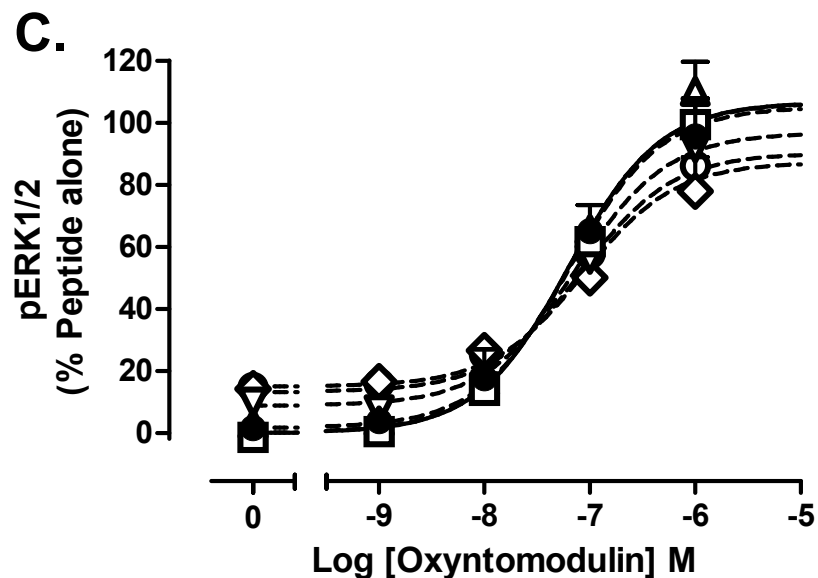
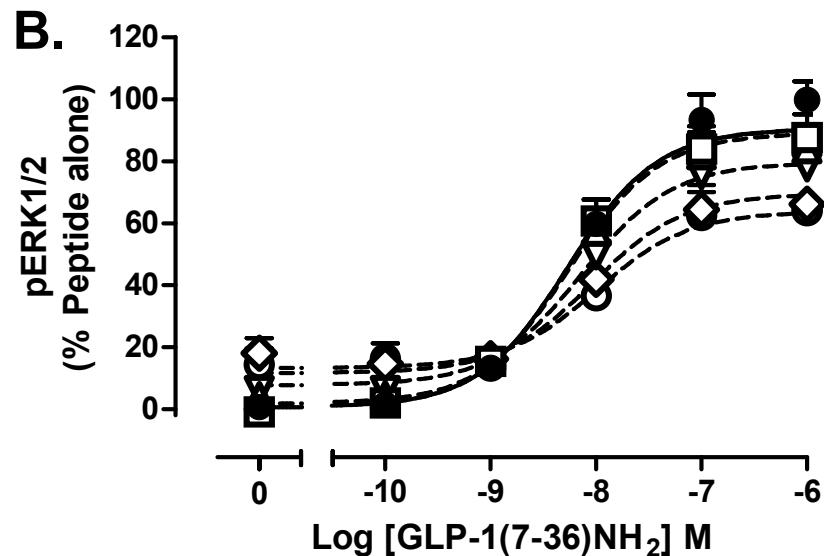
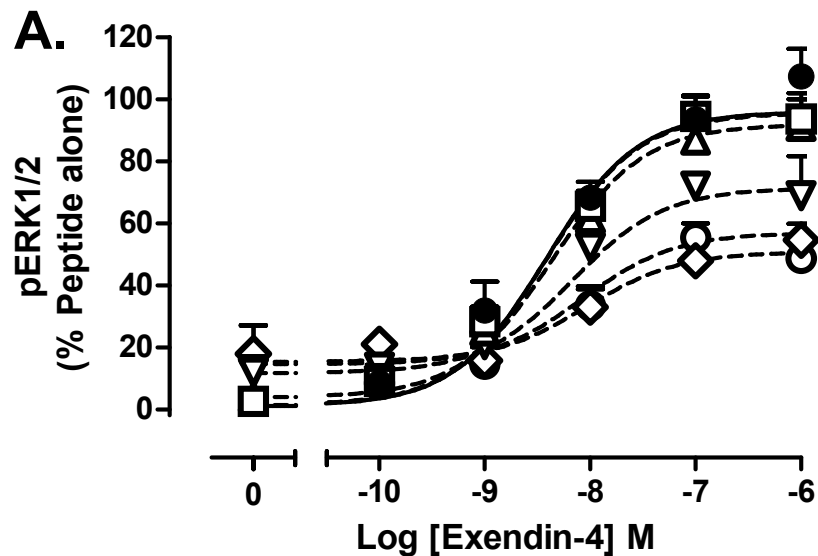


[Compound 2] ● 0 □ 10 nM ▲ 0.1 μM ▼ 1 μM ◇ 10 μM ○ 30 μM

Supplementary figure 4

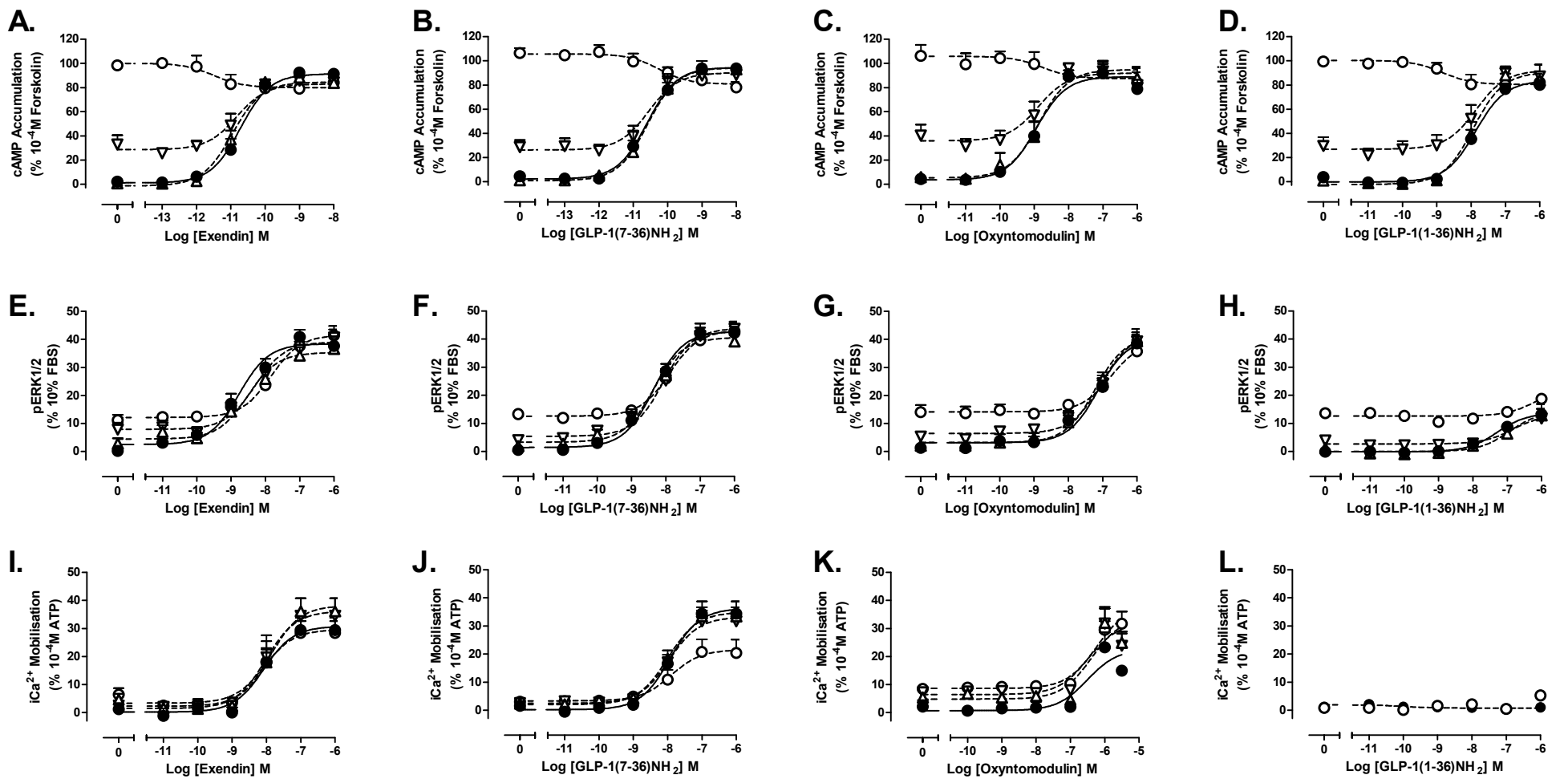


Supplementary figure 5



[Compound 2] ● 0 □ 0.1 μM ▲ 1 μM ▼ 10 μM ◇ 30 μM ○ 56 μM

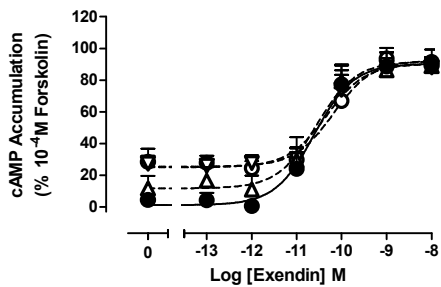
Supplementary figure 6



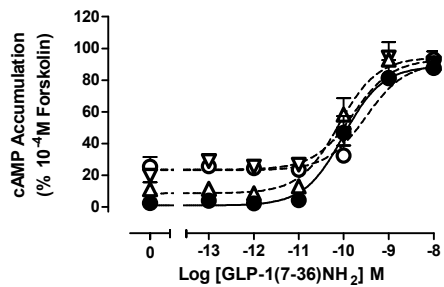
[BMS21] ● 0 ▲ 10 nM ▼ 0.1 μM ○ 1 μM

Supplementary figure 7

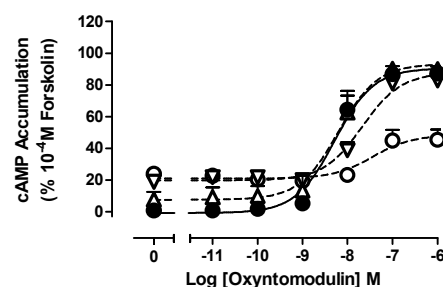
A.



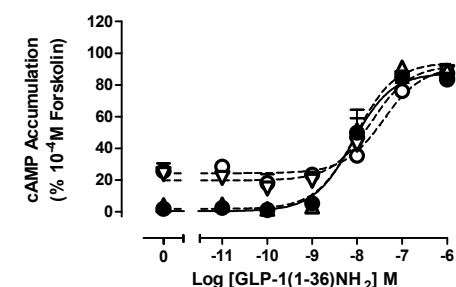
B.



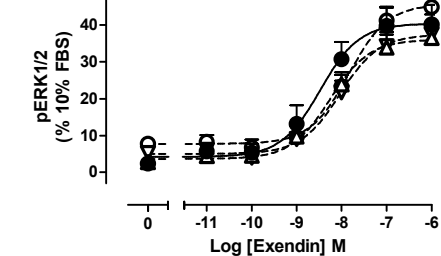
C.



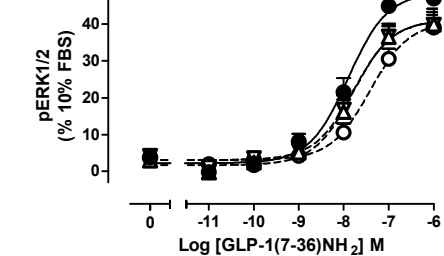
D.



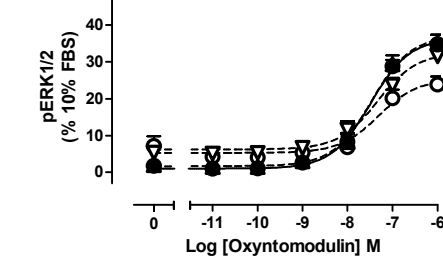
E.



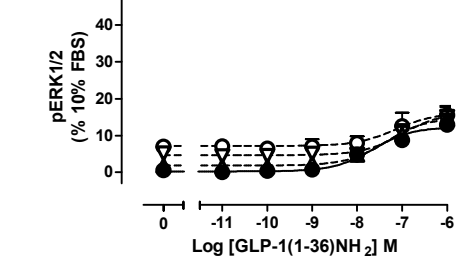
F.



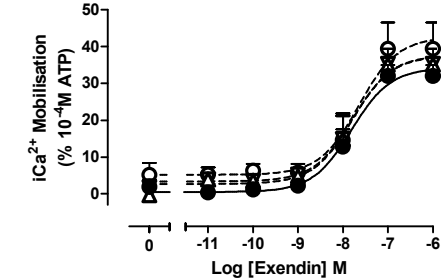
G.



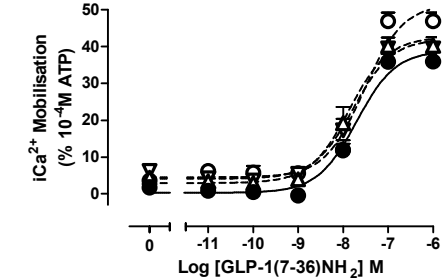
H.



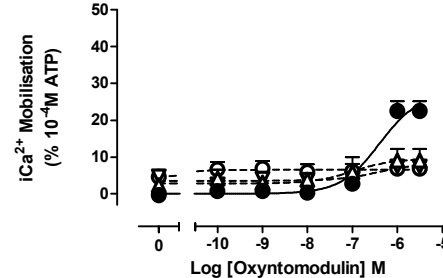
I.



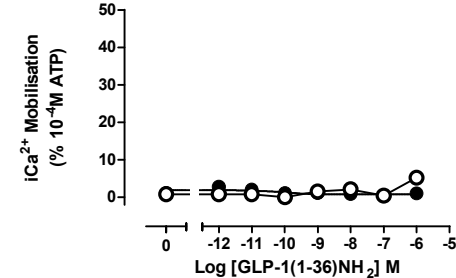
J.



K.



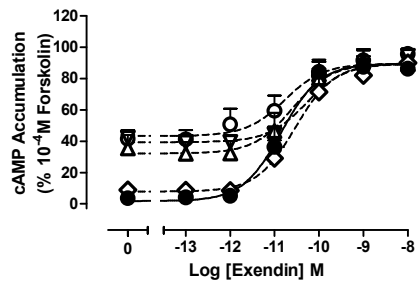
L.



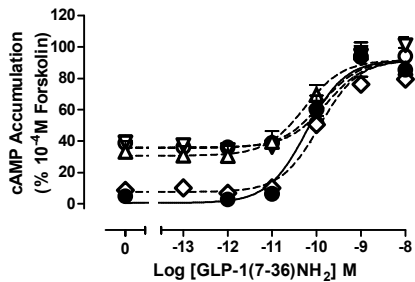
[Boc5] ● 0 ▲ 0.1 μ M ▼ 1 μ M ○ 10 μ M

Supplementary figure 8

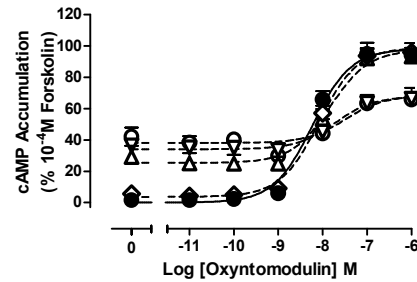
A.



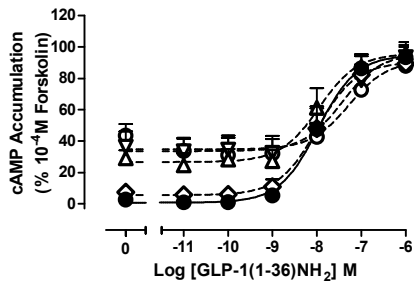
B.



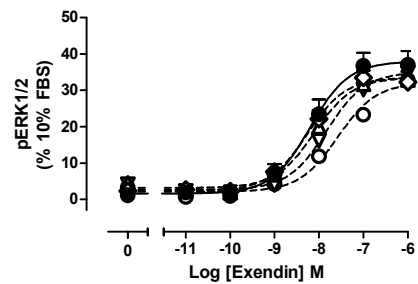
C.



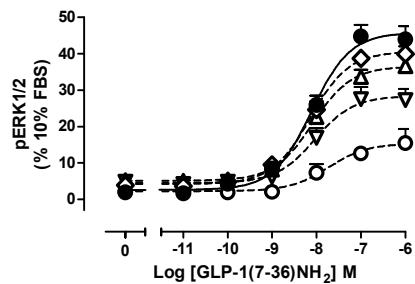
D.



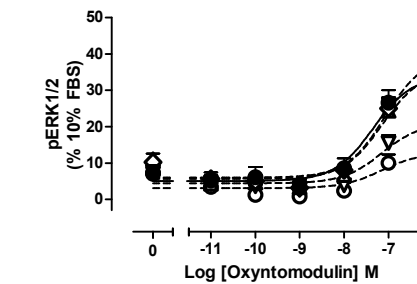
E.



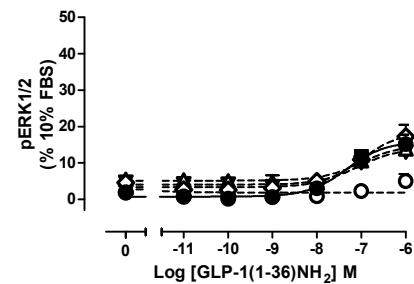
F.



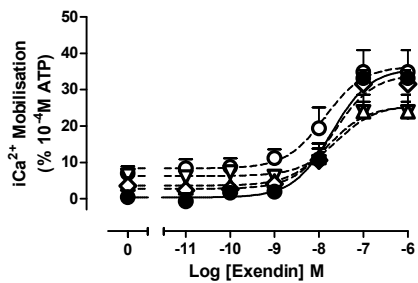
G.



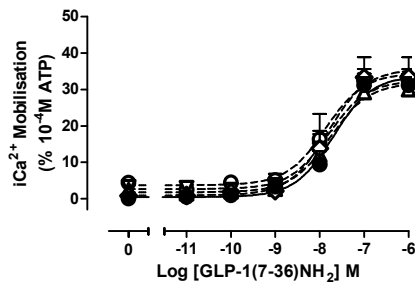
H.



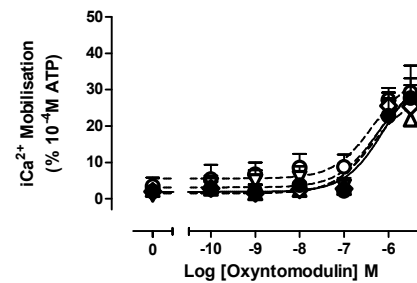
I.



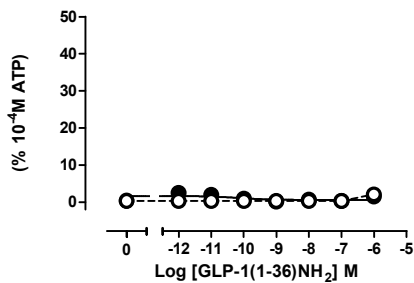
J.



K.



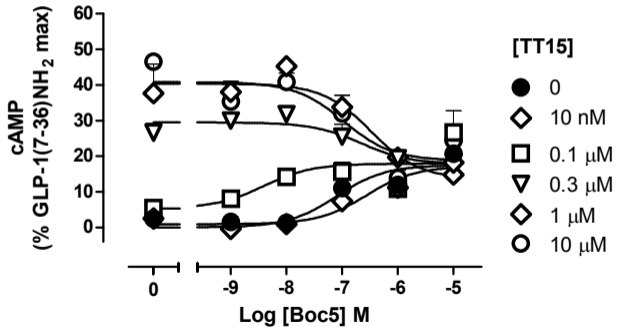
L.



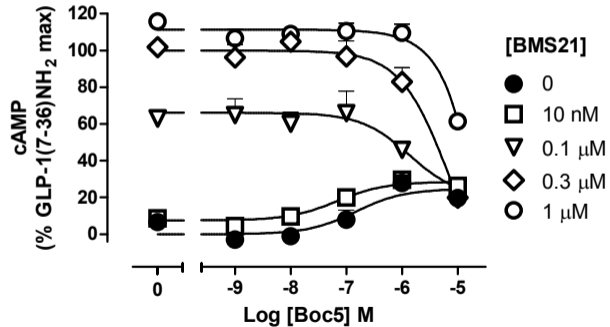
[TT15] ● 0 ◇ 0.1 μM ▲ 1 μM ▼ 10 μM ○ 30 μM

Supplementary figure 9

A.



B.



C.

